

# Analysis of Vibroarthrographic Signals with Features Related to Signal Variability and Radial-Basis Functions

RANGARAJ M. RANGAYYAN<sup>1</sup> and YUNFENG WU<sup>2</sup>

<sup>1</sup>Department of Electrical and Computer Engineering, Schulich School of Engineering, University of Calgary, Calgary, AB, Canada T2N 1N4; and <sup>2</sup>Beijing University of Posts and Telecommunications, 10 Xi Tu Cheng Road, Haidian District, Beijing 100876, China

(Received 30 October 2007; accepted 4 November 2008; published online 18 November 2008)

**Abstract**—Knee-joint sounds or vibroarthrographic (VAG) signals contain diagnostic information related to the roughness, softening, breakdown, or the state of lubrication of the articular cartilage surfaces. Objective analysis of VAG signals provides features for pattern analysis, classification, and noninvasive diagnosis of knee-joint pathology of various types. We propose parameters related to signal variability for the analysis of VAG signals, including an adaptive turns count and the variance of the mean-squared value computed during extension, flexion, and a full swing cycle of the leg, for the purpose of classification as normal or abnormal, that is, screening. With a database of 89 VAG signals, screening efficiency of up to 0.8570 was achieved, in terms of the area under the receiver operating characteristics curve, using a neural network classifier based on radial-basis functions, with all of the six proposed features. Using techniques for feature selection, the turns counts for the flexion and extension parts of the VAG signals were chosen as the top two features, leading to an improved screening efficiency of 0.9174. The proposed methods could lead to objective criteria for improved selection of patients for clinical procedures and reduce healthcare costs.

**Keywords**—Knee-joint sounds, Mean-squared value, Radial-basis functions, Turns count, Vibroarthrography.

## INTRODUCTION: KNEE-JOINT PATHOLOGY AND VIBROARTHROGRAPHY

The vibroarthrographic (VAG) signal, representing the sound or vibration emitted from a knee joint during flexion or extension, is expected to be associated with pathological conditions in the joint.<sup>5</sup> The application of digital signal processing and pattern classification techniques to VAG signals has been shown to provide indicators of the roughness, softening, breakdown, or the state of lubrication of the articular

cartilage surfaces, leading to noninvasive diagnosis of pathology<sup>3,10,12,13,16,20,22,23,25–27</sup>; see Rangayyan and Wu<sup>23</sup> for a recent detailed review. Detection of knee-joint pathology using VAG signals could reduce the need for diagnostic surgery; such a procedure could also find use in monitoring joint function and cartilage deterioration over time, as well as in the analysis of the effects of treatment and the functional integrity of prosthetic devices.

A significant portion of the patients who undergo arthroscopy have been observed to be free of any abnormality of the joint.<sup>15</sup> Due to the limitations in the application of advanced imaging techniques, such as computed tomography (CT) and magnetic resonance imaging (MRI) to the diagnosis of knee-joint pathology, there is renewed interest, among orthopedic surgeons and related specialists, in the use of VAG signals for noninvasive screening of patients presenting with complaints related to the knee joint, prior to the recommendation of arthroscopic examination. In order to address this need, we are interested in developing a screening tool for use in the clinic of a physician or an orthopedic specialist. Toward this end, we investigate the use of parameters that characterize the variability or activity present in VAG signals for normal-vs.-abnormal classification, that is, screening.<sup>24</sup>

## METHODS

### *VAG Signal Data Acquisition*

Each subject sat on a rigid table in a relaxed position with the leg being tested freely suspended in air. The VAG signal was recorded by placing an accelerometer (model 3115a, Dytran, Chatsworth, CA) at the mid-patella position of the knee as the subject swung the leg over an approximate angle range of 135° (approximately full flexion) to 0° (full extension) and back to 135° in 4 s.<sup>14,22</sup> The transducer has a nominal

Address correspondence to Rangaraj M. Rangayyan, Department of Electrical and Computer Engineering, Schulich School of Engineering, University of Calgary, Calgary, AB, Canada T2N 1N4. Electronic mail: ranga@ucalgary.ca, y.wu@ieee.org

sensitivity of 10 mV/G at 100 Hz, and a 3-dB bandwidth of 0.66–12,000 Hz. The subjects were provided verbal directions to complete the flexion–extension–flexion cycle in a period as close to 4 s as possible, with equal durations of 2 s for each of flexion and extension. The first half (approximately) of each VAG signal corresponds to extension, and the second half to flexion of the leg. Informed consent was obtained from each subject. The experimental protocol was approved by the Conjoint Health Research Ethics Board of the University of Calgary.

The VAG signal was prefiltered (10 Hz to 1 kHz) and amplified before digitizing at a sampling rate of 2 kHz. Each signal was normalized to the amplitude range [0, 1]. Figure 1 shows examples of normal and abnormal VAG signals. The abnormal signal exhibits a higher degree of overall variability, activity, or complexity than the normal signal.

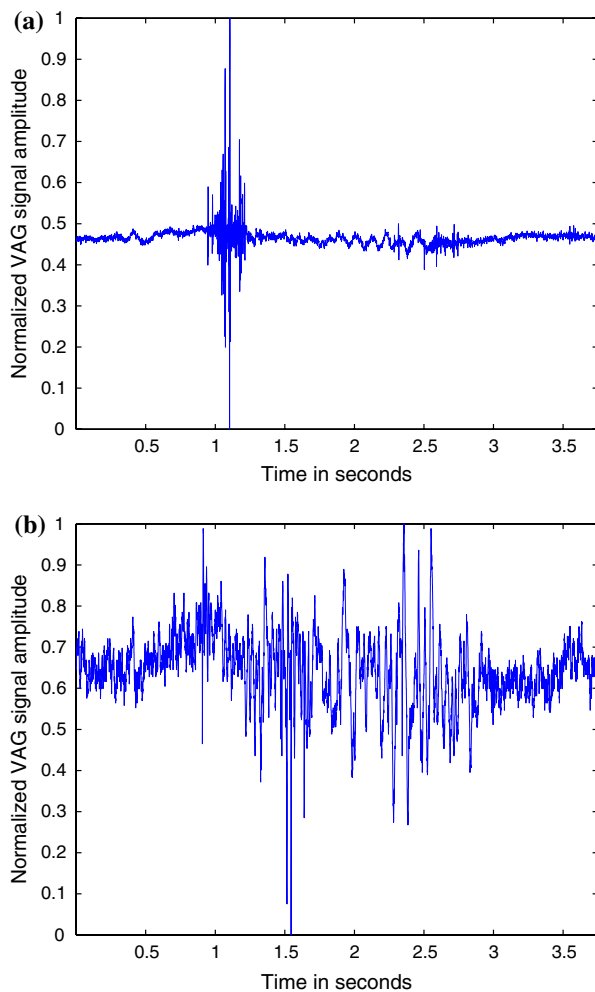


**FIGURE 1.** VAG signal examples: (a) of a normal subject; (b) of a patient with knee-joint pathology. The amplitudes have been normalized to the range [0, 1].

The database used in the present study consists of 89 signals, with 51 from normal volunteers and 38 from subjects with knee-joint pathology. The normals were established by clinical examination and history. The abnormal signals were collected from symptomatic patients scheduled to undergo arthroscopy independent of the VAG studies. The abnormal signals include chondromalacia of different grades at the patella, meniscal tear, tibial chondromalacia, and anterior cruciate ligament injuries, as confirmed during arthroscopic examination. The dataset available is not adequate to permit classification of the signals into various types or stages of pathology. The present study is aimed at screening only, that is, normal vs. abnormal classification.

As compared to previous related studies,<sup>12,13,22</sup> the dataset used in the present study lacks one abnormal VAG signal due to corruption of the data. The present study uses the same dataset as that used in a few recent studies.<sup>20,23,27</sup>

#### Feature Extraction from VAG Signals

VAG signals associated with knee-joint pathology have been observed to demonstrate a larger extent of variability over the duration of a swing cycle of the leg than normal VAG signals.<sup>14,19</sup> In order to characterize this property of the VAG signals, which could be lost in analysis based upon adaptive segments of the signals, Moussavi *et al.*<sup>19</sup> proposed a feature computed as the variance of the means of the segments of a given VAG signal; the signals were initially segmented adaptively using a recursive least squares (RLS) algorithm. In addition, VAG signals generated during extension (approximately the first half of the duration of each signal recorded according to the protocol described in section “VAG Signal Data Acquisition” and illustrated in Fig. 1) have been observed to bear more discriminant information than those related to flexion, due to increased loading of the knee joint during the former phase of swinging movement of the leg than the latter.<sup>14</sup> Taking these observations into consideration, in the present work, we first split each given VAG signal into two halves, with the first part corresponding to extension and the second part to flexion of the leg, and analyze them separately. In order to take into account the overall variability of a given VAG signal, we also analyze the signal over the full swing cycle.

In order to characterize the larger variability in abnormal VAG signals, as compared to normal VAG signals, the standard deviation or variance of the signals could be used. A measure of the complexity of a signal  $x$  is given by form factor (FF), which was originally defined by Hjorth<sup>7–9</sup>; see also Rangayyan.<sup>21</sup>

FF is defined as  $FF = \frac{\sigma_{x'} / \sigma_{x''}}{\sigma_{x'} / \sigma_x}$ , where  $\sigma$  stands for the standard deviation, and  $x'$  and  $x''$  are the first and second derivatives of the signal (or segment)  $x$ . We have shown that FF can provide good classification performance in discriminating between normal and abnormal VAG signals.<sup>20,23</sup> However, it should be noted that the standard deviation is affected by noise and outliers in signal values; in addition, the derivatives of the signal used to compute FF would contain amplified versions of the noise present in the original signals.

In the present work, we take a different approach: we compute the mean-squared (MS) values of a given VAG signal in fixed-duration segments of 5 ms each, and then compute the variance of the values of the parameter over the entire duration of the signal (labeled as VMS). The same procedure is applied to the first half (extension) and the second half (flexion) of the

VAG signal, resulting in the corresponding parameters labeled as VMS1 for the first half, and VMS2 for the second half. Note that the VMS values represent the variability (variance) of power in the signal. Figure 2 illustrates the variation of the mean-squared value, computed in nonoverlapping windows of duration 5 ms each, for the VAG signals in Fig. 1. Two additional VAG signals are shown in Figs. 3 and 4 along with the associated mean-squared values. It is evident that the abnormal signals have greater variation of power than the normal signals.

A different indication of the variability of a signal above a certain threshold is given by *turns count* (TC), originally proposed by Willison<sup>29</sup> for the analysis of electromyographic (EMG) signals; see also Rangayyan.<sup>21</sup> The procedure involves the detection of the number of spikes, swings, or changes in amplitude larger than a certain threshold. Instead of counting zero-crossings, the

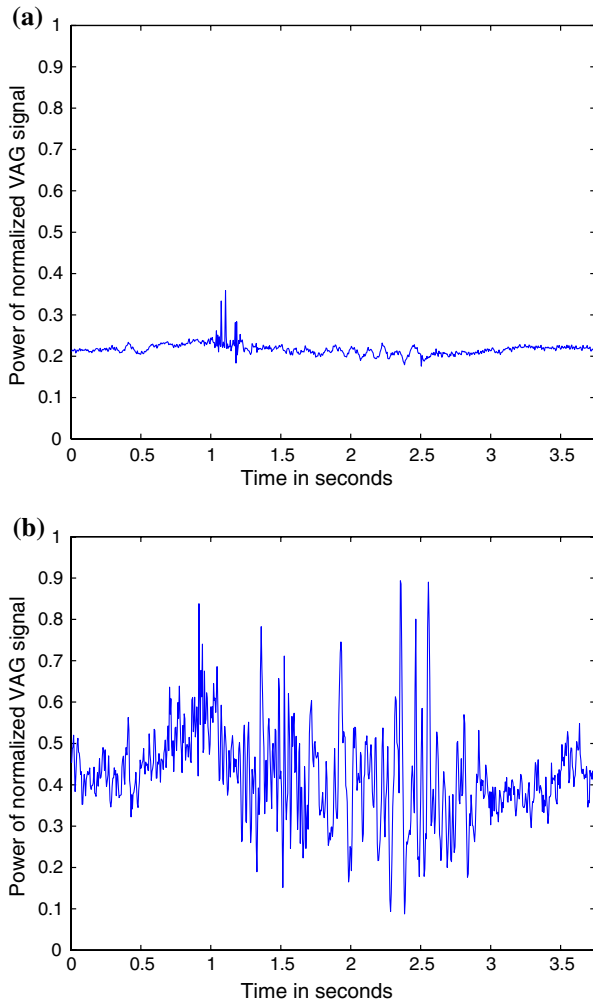


**FIGURE 2.** Illustration of the variation of the mean-squared value, computed in nonoverlapping windows of duration 5 ms each, for the VAG signals in Fig. 1: (a) of a normal subject; (b) of a patient with knee-joint pathology.

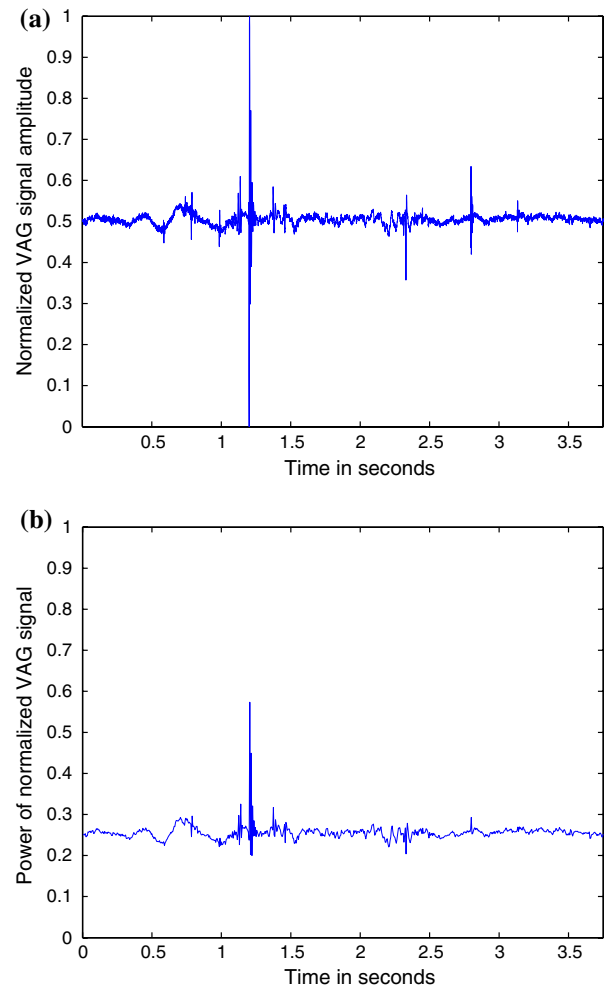


**FIGURE 3.** (a) VAG signal of a normal subject. (b) Plot illustrating the variation of the mean-squared value, computed in nonoverlapping windows of duration 5 ms each, for the VAG signal in (a).

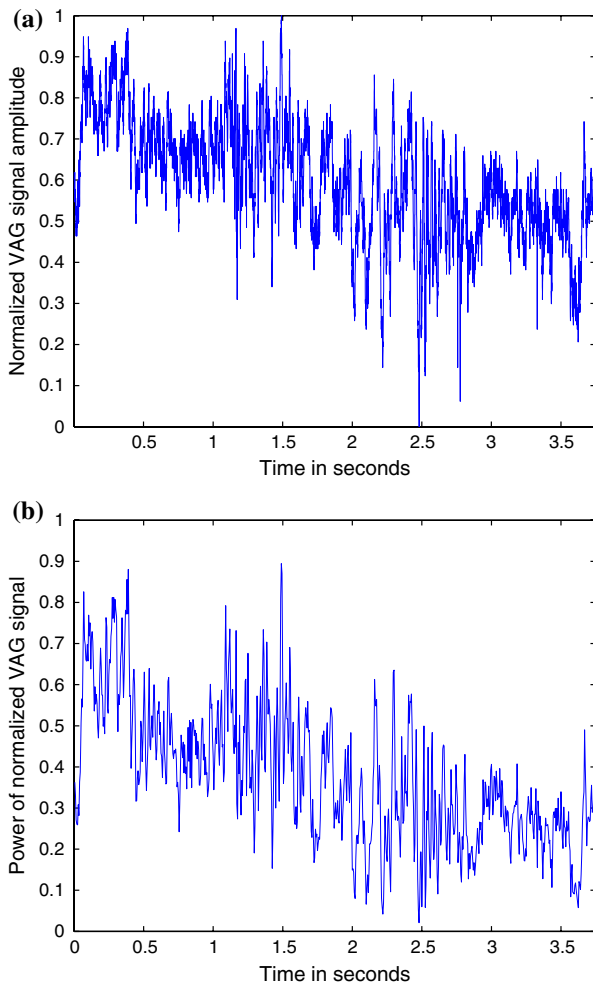


**FIGURE 4.** (a) VAG signal of a subject with a pathological knee joint. (b) Plot illustrating the variation of the mean-squared value, computed in nonoverlapping windows of duration 5 ms each, for the VAG signal in (a).

method checks the significance of each change in phase, direction, or slope in the signal, called a *turn*. Only those turns that are greater than the specified threshold are counted, in order to avoid the effects of noise. In contrast, a zero-crossing detector would be susceptible to the effects of noise. The TC method is related to a test for randomness.<sup>1,11,21</sup> Willison<sup>29</sup> showed that EMG signals of patients with myopathy have higher values of TC than signals of normal subjects at comparable levels of volitional effort.

In the present work, we compute values of TC for the entire duration of a given VAG signal, as well as for the first half (extension) and the second half (flexion) of the VAG signal, labeled as TC, TC1, and TC2, respectively. The threshold to determine the significance of a turn is computed adaptively for each signal as  $0.5\sigma_V$ , where  $\sigma_V$  is the standard deviation of the VAG signal being analyzed (computed over its entire

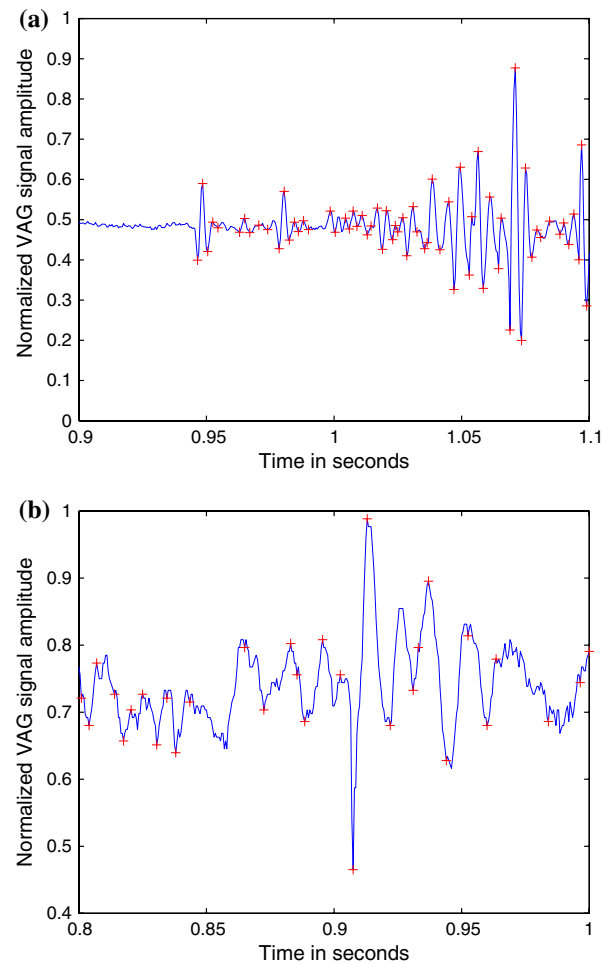


**FIGURE 5.** Illustration of the detection of turns in parts of the VAG signals in Fig. 1: (a) of a normal subject; (b) of a patient with knee-joint pathology. Significant turns detected have been labeled with red plus symbols. The threshold used to identify significant turns is adaptive, proportional to the standard deviation of the signal being analyzed.

duration, extension, or flexion for TC, TC1, or TC2, respectively).

Figure 5 illustrates examples of detection of turns in segments of the VAG signals in Fig. 1. Two additional examples, using segments from a normal and an abnormal VAG signal, are shown in Fig. 6 to further illustrate the detection of turns. The variance of a normal VAG signal is expected to be lower than that of an abnormal signal; as a consequence, the use of an adaptive threshold proportional to  $\sigma_V$  is expected to lead to larger counts for normal signals than for abnormal signals, for a given interval of time.

#### Feature Selection and Pattern Classification

Receiver operating characteristics (ROC) curves were generated for each feature using the software tool ROCKIT provided by the University of Chicago.<sup>17,18</sup>

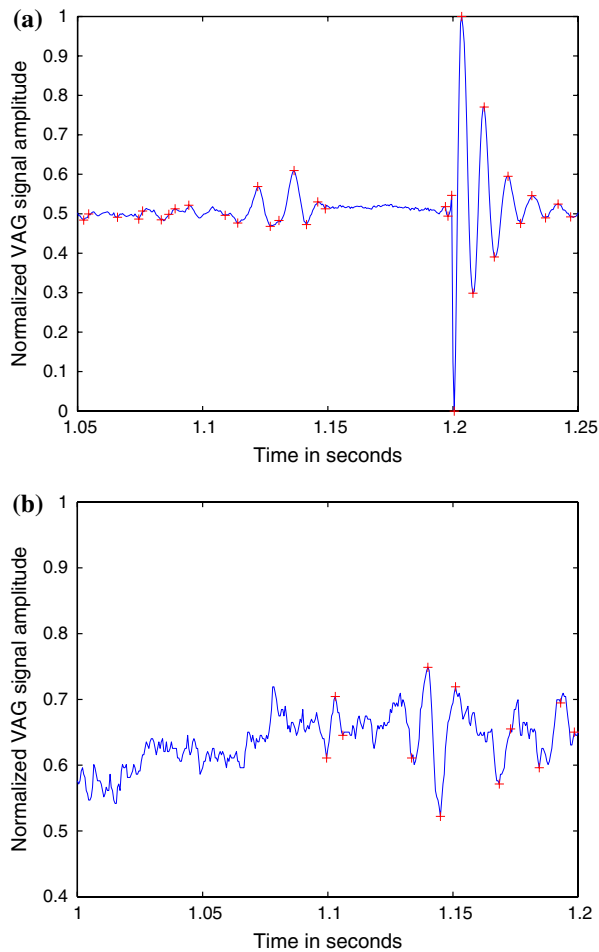


**FIGURE 6.** Illustration of the detection of turns in parts of two additional VAG signals: (a) of a normal subject; (b) of a patient with knee-joint pathology. Significant turns detected have been labeled with red plus symbols. The threshold used to identify significant turns is adaptive, proportional to the standard deviation of the signal being analyzed.

The area ( $A_z$ ) under the ROC curve was derived to serve as a measure of the overall classification performance in each experiment.

The six features computed were analyzed for their individual discriminant capability using their  $A_z$  values. The features were also analyzed for the statistical significance of the differences between the normal and abnormal categories by applying the  $t$ -test and deriving the  $p$ -values.<sup>28</sup> The sequential forward selection procedure was applied to rank-order the features.

Classification experiments were conducted by using several neural networks with radial-basis functions (RBF),<sup>6</sup> using the full set of features and the leave-one-out (LOO) procedure for cross validation.<sup>4</sup> An RBF network (RBFN) with a feed-forward hidden layer applies a nonlinear transformation from the input space to a high-dimensional hidden space, and then produces separable responses through a linear output

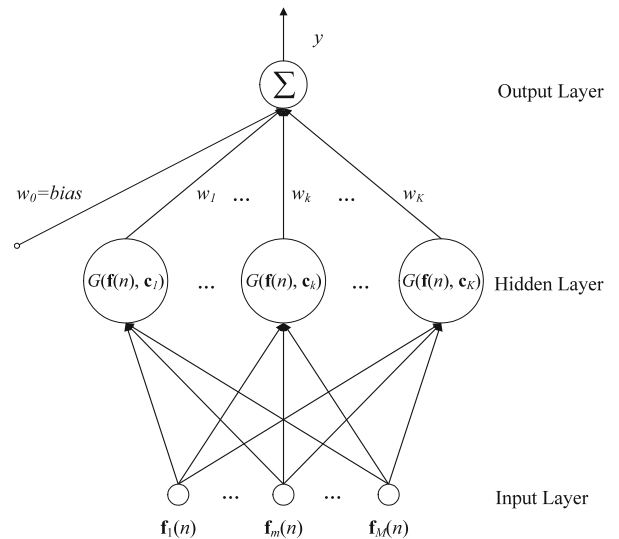


**FIGURE 7.** Schematic representation of the RBF network used for the classification of VAG signals. The inputs to the RBFN,  $f_1(n), f_2(n), \dots, f_M(n)$ , are the  $M$  components of the feature vector  $f(n)$  of a VAG signal to be classified. The hidden layer has  $K$  neurons.  $G(f(n), c_k)$  is the RBF of the  $k$ th neuron with center  $c_k$  and weight  $w_k$ .

transformation; see Fig. 7 for an illustration of the generic architecture of an RBFN. The results may be used to classify the signals by applying a threshold, or a sliding threshold may be applied to generate an ROC curve.

A difficulty in the design of an RBFN is the selection of the centers. Improper selection of the centers leads to a relatively large network with high computational complexity. In the present work, we applied the orthogonal least-squares (OLS) method,<sup>2</sup> which is a systematic method for center selection that can significantly reduce the size of the RBFN. See Rangayyan and Wu<sup>23</sup> for more details on the RBFN.

The details of the RBFN used in the present work are as follows: The input layer included  $M = 2$  to  $M = 6$  nodes to accept various sets of features extracted from each VAG signal. The spread parameter was varied over the range  $[1, 6]$ , and the number of hidden nodes was varied over the range  $[1, 30]$ . The resulting output values were used to derive ROC curves and the associated  $A_z$  values using ROCKIT. For the sake of comparison, classification experiments were also conducted using Fisher linear discriminant analysis (FLDA).<sup>4</sup>

## RESULTS

Table 1 lists the mean and standard deviation values of the six features computed for the 89 VAG signals tested. It is evident that the abnormal signals possess

**TABLE 1. Mean and standard deviation (SD) of the proposed features for the normal (51) and abnormal (38) VAG signals.**

Feature	Mean $\pm$ SD (normal signals)	Mean $\pm$ SD (abnormal signals)
TC	1686.50 $\pm$ 828.78	1216.80 $\pm$ 830.21
TC1	898.24 $\pm$ 395.13	635.24 $\pm$ 405.65
TC2	939.90 $\pm$ 417.67	639.66 $\pm$ 434.42
VMS	0.0058 $\pm$ 0.0062	0.0123 $\pm$ 0.0138
VMS1	0.0052 $\pm$ 0.0059	0.0104 $\pm$ 0.0124
VMS2	0.0052 $\pm$ 0.0060	0.0111 $\pm$ 0.0121

TC, TC1, TC2: Turns count for the full duration, the first half (extension), and the second half (flexion), respectively. VMS, VMS1, VMS2: Variance of the mean-squared value for the full duration, the first half (extension), and the second half (flexion), respectively.

higher variance of power (VMS) than the normal signals, as expected. Because of the use of an adaptive threshold, proportional to the standard deviation of the signal being processed, the abnormal signals have lower turns counts than the normal signals. The use of fixed thresholds to determine the significance of turns led to poor discrimination between normal and abnormal VAG signals; this could be due to variations in the signal acquisition procedure and normalization of the signal amplitude.

The separability of the individual features is indicated by the following  $p$ -values, obtained using the  $t$ -test: TC: 0.0098, TC1: 0.0028, TC2: 0.0014, VMS: 0.0032, VMS1: 0.0112, and VMS2: 0.0032. The  $p$ -values indicate that all of the features possess statistically highly significant differences ( $p < 0.01$ ) between the normal and abnormal VAG signals, except VMS1 which possesses significant difference ( $0.01 < p < 0.05$ ). Individually, the features gave the following  $A_z$  values: TC: 0.6551, TC1: 0.6808, TC2: 0.6742, VMS: 0.6935, VMS1: 0.6708, and VMS2: 0.6744. The results are summarized in Table 2.

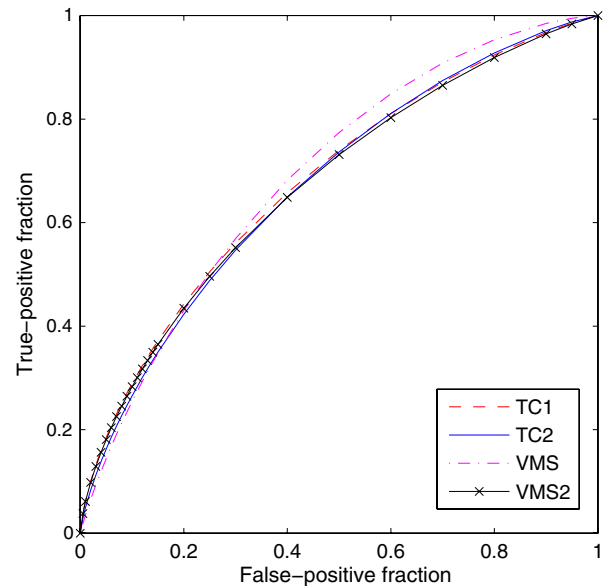
The application of sequential forward selection resulted in different results depending upon the criterion used. Using  $A_z$  values, the rank-ordered list of features is {VMS, TC1, VMS2, TC2, VMS1, TC}. Using the  $p$ -values, the rank-ordered list is {TC2, TC1, VMS2, VMS, TC, VMS1}.

The full set of the six features provided  $A_z = 0.6521$  with FLDA and  $A_z = 0.8570$  with the RBFN (spread = 4 with 16 hidden nodes), including the LOO procedure. The criterion for selecting the number of hidden nodes and the value of the spread parameter in the RBFN was the overall classification accuracy of the normal and abnormal signals. Use of the top two or four features selected based upon the  $A_z$  values led to poor results with FLDA and RBFN. Use of the top two or four features selected based upon the  $p$ -values provided poor results with FLDA, but improved

**TABLE 2. Statistical significance of separability ( $p$ -value) and classification performance (area  $A_z$  under the ROC curve and the associated standard error, SE) of the features used for the screening of VAG signals.**

Feature/classifier	$p$ -value	$A_z$	SE
TC	0.0098	0.6551	0.0583
TC1	0.0028	0.6808	0.0567
TC2	0.0014	0.6742	0.0570
VMS	0.0032	0.6935	0.0555
VMS1	0.0112	0.6708	0.0576
VMS2	0.0032	0.6744	0.0574
FLDA/LOO using all 6 features	N/A	0.6521	0.0579
FLDA/LOO using {TC1, TC2}	N/A	0.6352	0.0586
FLDA/LOO using {TC1, TC2, VMS, VMS2}	N/A	0.6352	0.0586
RBFN/LOO using all 6 features	N/A	0.8570	0.0481
RBFN/LOO using {TC1, TC2}	N/A	0.9174	0.0343
RBFN/LOO using {TC1, TC2, VMS, VMS2}	N/A	0.9174	0.0343

TC, TC1, TC2: Turns count for the full duration, the first half (extension), and the second half (flexion), respectively. VMS, VMS1, VMS2: Variance of the mean-squared value for the full duration, the first half (extension), and the second half (flexion), respectively. FLDA: Fisher linear discriminant analysis. LOO: Leave-one-out cross validation. RBFN: Classification using a neural network with radial-basis functions. N/A: not applicable.

**FIGURE 8. ROC plots for the individual features TC1, TC2, VMS, and VMS2. The corresponding areas under the ROC curves ( $A_z$ ) are 0.6808, 0.6742, 0.6935, and 0.6744, respectively. Due to similar classification performance, the ROC plots overlap significantly with one another. See Table 2 for further details.**

results of  $A_z = 0.9174$  with the RBFN (spread = 4 with 15 hidden nodes), including the LOO procedure. The results are summarized in Table 2. See Figs. 8 and 9 for the ROC plots of selected experiments.

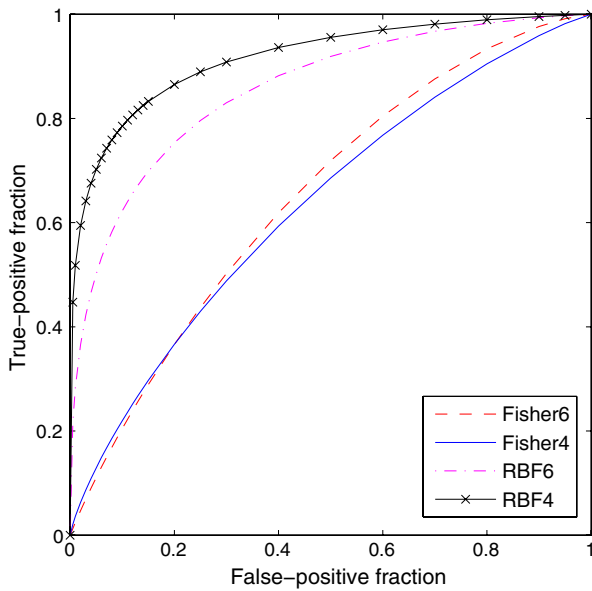


**FIGURE 9.** ROC plots for the FLDA (labeled as Fisher6 and Fisher4) and RBFN classifiers (RBF6 and RBF4), including the LOO procedure, using the sets of features {TC, TC1, TC2, VMS, VMS1, VMS2} and {TC1, TC2, VMS, VMS2}. The corresponding areas under the ROC curves ( $A_z$ ) are Fisher6: 0.6521, Fisher4: 0.6352, RBF6: 0.8570, and RBF4: 0.9174, respectively. See Table 2 for further details.

The results indicate that the proposed adaptive turns count and the variance of the power (VMS) over the extension and flexion parts as well as over the entire swing cycle can yield good levels of accuracy in screening VAG signals. This agrees with the observations in previous studies,<sup>10,14,19,26</sup> where power-related parameters of VAG signals have shown good discriminant capabilities. In particular, use of the feature set {TC1, TC2} provided the best result, with  $A_z = 0.9174$ . However, the features are not linearly separable to a good degree of classification accuracy, and require a nonlinear classifier; the RBFN classifier used has provided a high classification performance.

## DISCUSSION AND CONCLUSION

The proposed methods have shown good performance in noninvasive screening for articular cartilage pathology. Specifically, the turns count and variance of the mean-squared values (power), computed separately for the flexion and extension parts of the VAG signals, have provided high screening accuracy. The features relate to signal variability, and represent the overall variation in a given VAG signal over a swing cycle. Abnormal VAG signals have been clinically observed to possess larger variability than normal VAG signals: this distinguishing characteristic is captured by the proposed feature VMS. The present work is focused on

screening VAG signals (as normal or abnormal). More specific features would be required to identify different types of pathology.

In comparison with the results reported in previous studies on the analysis of VAG signals with the same dataset as in the present study (except for the loss of one signal), the results obtained in the present study are important in that the proposed parameters, derived from the VAG signals with no segmentation other than splitting the duration of each signal in halves, have provided screening accuracies comparable to or better than those obtained with more sophisticated methods, such as autoregressive modeling (68.9 and 70%),<sup>13,22</sup> cepstral coefficients (75.6%),<sup>22</sup> time-frequency distributions (68.9%),<sup>12</sup> and wavelet packet decomposition (79.8%).<sup>27</sup> In our most recent related study,<sup>23</sup> the best screening performance obtained was  $A_z = 0.8172$  using the same dataset as in the present study with form factor, skewness, kurtosis, and entropy as the features, and an RBFN classifier; the present work has yielded a higher performance with  $A_z = 0.9174$ .

The proposed methods do not require clinical information regarding the patient, reports related to auscultation of the knee joint, or clinical interpretation of the VAG signals. The removal of the segmentation step overcomes the need to estimate the joint angle corresponding to the pathology as observed during clinical examination, auscultation, or arthroscopy.

The parameters of the RBFN classifier need to be determined by conducting experiments with a training set; however, once trained, the computational requirements of the RBFN are not large in a classification task. Further work will be conducted on the selection of high-performance combinations of features and the application of advanced nonlinear and kernel-based classifiers,<sup>20</sup> which could lead to improved results.

The relatively simple signal processing techniques that have been used in the present work could lead to a practical approach for the analysis of the nonstationary VAG signals. We intend to develop a simple computational tool for use in the clinic of a physician or an orthopedic specialist. Selection of patients based on objective criteria for clinical procedures such as arthroscopy could reduce costs to the healthcare system and the patient.

## ACKNOWLEDGMENTS

This work was supported by the Doctoral Program Foundation of the Ministry of Education of China under Grant No. 20060013007 awarded to Y. F. Wu, and by the University of Calgary in the

form of a “University Professorship” awarded to R. M. Rangayyan. R. M. Rangayyan is a Visiting Professor at the Beijing University of Posts and Telecommunications. We thank Yachao Zhou and Xiaoxuan Zhu for technical assistance and review of this paper.

## REFERENCES

- <sup>1</sup>Challis, R. E., and R. I. Kitney. Biomedical signal processing (in four parts). Part 1. Time-domain methods. *Med. Biol. Eng. Comput.* 28:509–524, 1990.
- <sup>2</sup>Chen, S., C. F. N. Cowan, and P. M. Grant. Orthogonal least squares learning algorithm for radial basis function networks. *IEEE Trans. Neural Netw.* 2(2):302–309, 1991.
- <sup>3</sup>Chu, M. L., I. A. Gradsar, and L. D. Zavodney. Possible clinical application of a noninvasive monitoring technique of cartilage damage in pathological knee joints. *J. Clin. Eng.* 3(1):19–27, 1978.
- <sup>4</sup>Duda, R. O., and P. E. Hart. *Pattern Classification and Scene Analysis*. New York, NY: Wiley, 1973.
- <sup>5</sup>Frank, C. B., R. M. Rangayyan, and G. D. Bell. Analysis of knee sound signals for non-invasive diagnosis of cartilage pathology. *IEEE Eng. Med. Biol. Mag.* 9(1):65–68, 1990.
- <sup>6</sup>Haykin, S. *Neural Networks: A Comprehensive Foundation*. 2nd ed. Englewood Cliffs, NJ: Prentice-Hall PTR, 2002.
- <sup>7</sup>Hjorth, B. EEG analysis based on time domain properties. *Electroencephalogr. Clin. Neurophysiol.* 29:306–310, 1970.
- <sup>8</sup>Hjorth, B. The physical significance of time domain descriptors in EEG analysis. *Electroencephalogr. Clin. Neurophysiol.* 34:321–325, 1973.
- <sup>9</sup>Hjorth, B. Time domain descriptors and their relation to a particular model for generation of EEG activity. In: *CEAN: Computerised EEG Analysis*, edited by G. Dolce and H. Künkel. Stuttgart, Germany: Gustav Fischer, 1975, pp. 3–8.
- <sup>10</sup>Jiang, C.-C., J.-H. Lee, and T.-T. Yuan. Vibration arthrometry in the patients with failed total knee replacement. *IEEE Trans. Biomed. Eng.* 47(2):218–227, 2000.
- <sup>11</sup>Kendall, M. *Time-Series*. 2nd ed. London, UK: Charles Griffin, 1976.
- <sup>12</sup>Krishnan, S., R. M. Rangayyan, G. D. Bell, and C. B. Frank. Adaptive time–frequency analysis of knee joint vibroarthrographic signals for noninvasive screening of articular cartilage pathology. *IEEE Trans. Biomed. Eng.* 47(6):773–783, 2000.
- <sup>13</sup>Krishnan, S., R. M. Rangayyan, G. D. Bell, C. B. Frank, and K. O. Ladly. Adaptive filtering, modelling, and classification of knee joint vibroarthrographic signals for non-invasive diagnosis of articular cartilage pathology. *Med. Biol. Eng. Comput.* 35:677–684, 1997.
- <sup>14</sup>Ladly, K. O., C. B. Frank, G. D. Bell, Y. T. Zhang, and R. M. Rangayyan. The effect of external loads and cyclic loading on normal patellofemoral joint signals. *Spl. Iss. Biomed. Eng. Def. Sci. J. (India)* 43:201–210, 1993.
- <sup>15</sup>Lund, F., and B. E. Nilsson. Arthroscopy of the patellofemoral joint. *Acta Orthop. Scand.* 51:297–302, 1980.
- <sup>16</sup>McCoy, G. F., J. D. McCrea, D. E. Beverland, W. G. Kernohan, and R. A. B. Mollan. Vibration arthrography as a diagnostic aid in diseases of the knee. *J. Bone Joint Surg.* 69-B(2):288–293, 1987.
- <sup>17</sup>Metz, C. E. Basic principles of ROC analysis. *Sem. Nucl. Med.* VIII(4):283–298, 1978.
- <sup>18</sup>Metz, C. E., and L. Pesce. Readings in ROC Analysis, with Emphasis on Medical Applications. Available at [www.radiology.uchicago.edu/krl/KRL\\_ROC/ROC\\_analysis\\_by\\_topic4.htm](http://www.radiology.uchicago.edu/krl/KRL_ROC/ROC_analysis_by_topic4.htm). Chicago, IL: University of Chicago, 2006.
- <sup>19</sup>Moussavi, Z. M. K., R. M. Rangayyan, G. D. Bell, C. B. Frank, K. O. Ladly, and Y. T. Zhang. Screening of vibroarthrographic signals via adaptive segmentation and linear prediction modeling. *IEEE Trans. Biomed. Eng.* 43(1):15–23, 1996.
- <sup>20</sup>Mu, T., A. K. Nandi, and R. M. Rangayyan. Strict 2-surface proximal classification of knee-joint vibroarthrographic signals. In: *Proc. 29th Annual International Conference of the IEEE Engineering in Medicine and Biology Society*. Lyon, France: IEEE, pp. 4911–4914, August 2007.
- <sup>21</sup>Rangayyan, R. M. *Biomedical Signal Analysis—A Case-Study Approach*. New York, NY: IEEE and Wiley, 2002.
- <sup>22</sup>Rangayyan, R. M., S. Krishnan, G. D. Bell, C. B. Frank, and K. O. Ladly. Parametric representation and screening of knee joint vibroarthrographic signals. *IEEE Trans. Biomed. Eng.* 44(11):1068–1074, 1997.
- <sup>23</sup>Rangayyan, R. M., and Y. F. Wu. Screening of knee-joint vibroarthrographic signals using statistical parameters and radial basis functions. *Med. Biol. Eng. Comput.* 46(3):223–232, 2008.
- <sup>24</sup>Rangayyan, R. M., and Y. F. Wu. Screening of knee-joint vibroarthrographic signals using parameters of activity and radial-basis functions. In: *Proc. 21st IEEE Canadian Conference on Electrical and Computer Engineering*. Niagara Falls, Ontario, Canada: IEEE, pp. 57–60, May 2008.
- <sup>25</sup>Reddy, N. P., B. M. Rothschild, M. Mandal, V. Gupta, and S. Suryanarayanan. Noninvasive acceleration measurements to characterize knee arthritis and chondromalacia. *Ann. Biomed. Eng.* 23:78–84, 1995.
- <sup>26</sup>Reddy, N. P., B. M. Rothschild, E. Verrall, and A. Joshi. Noninvasive measurement of acceleration at the knee joint in patients with rheumatoid arthritis and spondyloarthropathy of the knee. *Ann. Biomed. Eng.* 29(12):1106–1111, 2001.
- <sup>27</sup>Umopathy, K., and S. Krishnan. Modified local discriminant bases algorithm and its application in analysis of human knee joint vibration signals. *IEEE Trans. Biomed. Eng.* 53(3):517–523, 2006.
- <sup>28</sup>Ware, J. H., F. Mosteller, F. Delgado, C. Donnelly, and J. A. Ingelfinger. P values. In: *Medical Uses of Statistics*, 2nd ed., edited by J. C. Bailar III and F. Mosteller. Boston: NEJM Books, 1992, pp. 181–200.
- <sup>29</sup>Willison, R. G. Analysis of electrical activity in healthy and dystrophic muscle in man. *J. Neurol. Neurosurg. Psychiatry* 27:386–394, 1964.